A High Density 400 W DC/DC Power Module with Integrated Planar Transformer and Half Bridge GaN IC

Bin Li
Navitas Semiconductor
Torrance, U. S.
bin.li@navitassemi.com

Xiucheng Huang
Navitas Semiconductor
Torrance, U. S.
xiucheng.huang@navitassemi.com

Jason Zhang
Navitas Semiconductor
Torrance, U. S.
jason.zhang@navitassemi.com

***Abstract*— The increasing popularity of gaming laptops, portable workstations, all-in-one computers, smart displays, and large screen OLED TVs has led to a rising demand for high-efficiency, high-density power supplies in the range of 300 W-500 W. Especially the all-in-one computer, smart display, and the large screen OLED TVs, they face form factor limitations, posing challenges for the overall thickness of the power supply. In this paper, an LLC resonant converter module is designed as the DC/DC stage of the power supply. By utilizing a highly integrated half bridge GaN power IC, the switching frequency of the DC/DC stage is boosted to over 500 kHz, enabling the design of a PCB-based transformer with an integrated resonant inductor. The prototype has a profile of only 8 mm, attains 21.5 kW/L power density (62.5 x 37.2 x 8 mm), which is far beyond the state-of-the-art design [1-3], with a peak efficiency of 98.1% and a full load (400 W) efficiency of 97.4%.**

Keywords—power converter module, half bridge GaN IC, high density, magnetic integration

I. INTRODUCTION

All-in-one computers and smart displays are gaining increasing popularity due to their space-saving and sleek appearance. Meanwhile, advancements in technology have led to a growing demand for large-sized OLED TVs, gaming laptops, and portable workstations among people. All these applications require power conversion from AC grid to low voltage DC output (20 V or 24 V). This power conversion usually consists of two stages. The first stage is a PFC converter, which performs power factor correction function and boosts the voltage to 400 VDC. The second stage is an isolated DC/DC converter, providing galvanic isolation while regulating the output voltage to the required level.

When examining the internal structure of Apple's latest studio display (Fig. 1) [4], which represents the most advanced technology available, the two-stage power supply can be identified: a Boost PFC stage followed by an LLC resonant converter as the DC/DC stage, as shown (Fig. 2). In the first stage, power factor correction is per-formed while transferring the AC utility power to a constant 380 V DC bus voltage. The second stage regulates the voltage and provides isolation, converting the 380 V bus voltage to a 20 V/24 V low voltage output for the subsequent stages. The Boost PFC operates at a switching frequency of approximately 65 kHz to achieve optimal efficiency and EMI performance, while the LLC resonant converter switches at a frequency of 100 kHz-150 kHz due to the lower switching loss.

Clearly the power supply occupies a significant portion of the space. Additionally, two large fans are present to dissipate the heat generated by the power supply and the A13 processor. Worth noting is the slim profile of the studio display, measuring only 18 mm in thickness [5]. Together with the board cuts out for the magnetics and capacitors, we can only imagine the requirements of the power supply in terms of footprint, thickness, and efficiency.

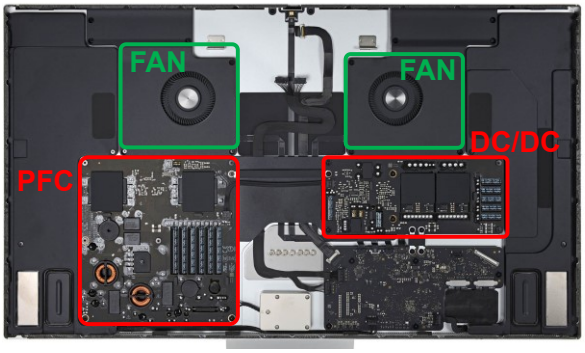

Fig. 1 Power supply inside Apple's studio display

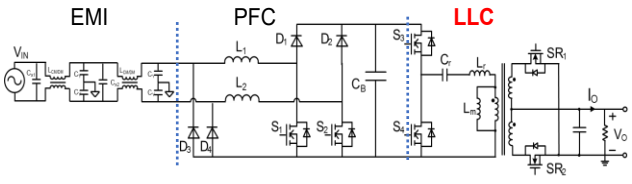

Fig. 2 A typical two stage architecture of the AC/DC power supply

In this paper, a high power density and high efficiency LLC resonant converter for the second stage is designed, which converts 400 VDC to 24 VDC. With the emerging wide bandgap materials, especially GaN, the switching speed of power converter can be improved significantly due to its much lower parasitic capacitance and zero reverse recovery [5-7]. And it becomes possible to adopt PCB base

planar transformer to shrink the area and thickness of the magnetics [8, 9]. In addition, the resonant inductor can be integrated into the transformer, which makes the system more concise and compact [10, 11].

Furthermore, by integrating two GaN power devices, their corresponding drivers, current sensing, level shifter and bootstrap all together in a 6 x 8mm QFN package, the GaN half bridge can greatly shrink the total footprint of the semiconductors and simply the system design.

In section II, the system structure design is given. Section III provides the design of the integrated planar transformer, including the 3D finite element analysis (FEA). Preliminary experimental results are in section IV, with summary and conclusion in section V.

II. SYSTEM STRUCTURE DESIGN USING HALF BRIDGE GAN POWER IC

A. *Half Bridge GaN IC*

The half bridge GaN power IC is a highly integrated power stage consisting of two GaN power devices in a half bridge configuration, along with two corresponding drivers, a level shifter to eliminate the need for an additional isolator and a bootstrap circuit to power up the high side [12].

Additional functions are also built into this IC [13].

1) Cycle-by-Cycle over current protection

During the low-side on-time of each switching cycle, should the peak current exceed the internal OCP threshold (1.9V, typical), the internal gate drive will turn the GaN power FET off quickly and truncate the on-time period to prevent damage from occurring to the IC. The IC will then turn on again at the next low-side PWM rising edge at the start of the next on-time period. This OCP feature self-protects the Gan power IC during each switching cycle against fast peak over current events and greatly increase the robustness and reliability of the system. This built-in circuit can safely turn off the GaN FET in less than 100ns.

2) Lossless current sensing

The GaN power IC incorporates a lossless current sensing by outputting a mirrored current through CS pin of the IC. It helps to obviate the necessity for sensing resistors in certain applications (Fig. 3), reducing system cost as well as system loss.

3) Tunable turn-on speed.

The turn on speed of both high side switch and low side switch can be tuned independently by adjusting the external resistor, giving designers the freedom to trade-off between switching speed and EMI performance.

All this features and functions are integrated into a 6 mm x 8 mm QFN package (as shown in Fig. 4). This high-level integration and significant reduction in component count and footprint make it possible to build a complete DC/DC converter module in a very compact formfactor.

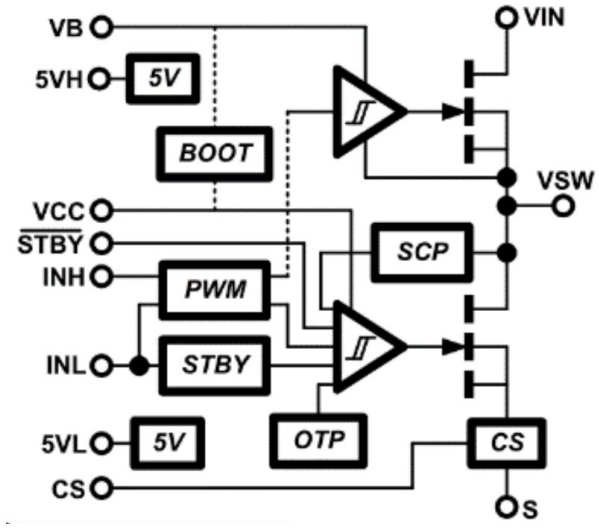

Fig. 3 Simplified schematic of half bridge GaN power IC.

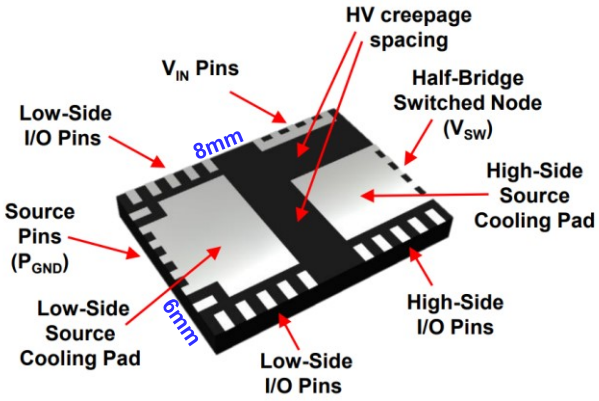

Fig. 4 Package and description of the half bridge GaN power IC.

The basic switching waveforms (Fig. 5) during resonant ZVS conditions (f_{sw} = 250 kHz, duty-cycle = 50%) include INH PWM input signal, VSW half-bridge switched node output, and output inductor current (IL). The switching performance shows excellent on/off control of the integrated high- and low-side GaN power FETs.

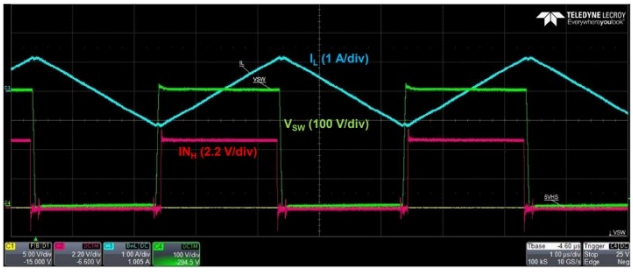

Fig. 5 Soft switching waveform of the half-bridge GaN power IC

B. System Structure Design

The proposed LLC converter structure is shown in Fig. 6. For application with hundreds of watts power, half bridge is commonly used on the primary side to save the cost and simply the system design. While on the secondary side center-type is the most popular due to easier driving of the synchronous rectifier (SR).

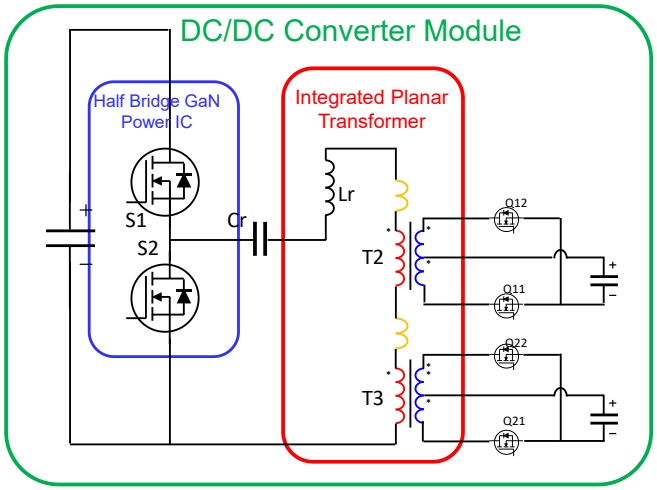

Fig. 6 LLC resonant converter with two transformers and two sets of output.

To handle the high output current, paralleling output is required to reduce the conduction loss. To determine the optimal number of output sets, losses need to be evaluated with different number of output sets.

$$P_{dr} = Q_g V_{gs} f_{sw} \tag{1}$$

$$P_{cond} = R_{dson}(T) \times I_{rms}^2 \tag{2}$$

$$P_{3rd} = V_f I_f t_{3rd} \times f_{sw} \tag{3}$$

Eq. (1), Eq. (2) and Eq. (4) represent the driving loss, conduction loss and the third quadrant conduction loss of the SR respectively, where

Q_g is the total gate charge of the SR,

V_{gs} is the gate driving voltage,

f_{sw} is the switching frequency,

$R_{dson}(T)$ is the on resistance scaled with temperature

I_{rms} is the RMS current flowing through the SR,

V_f, I_f and t_{3rd} are the forward voltage drop, current flowing the body diode and the time duration.

From these equations, we can see that driving loss and third quadrant conduction loss is related to switching frequency while conduction loss is related to output power.

The total loss is then calculated with different number of output sets. Consequently, the optimal number of output sets can be selected to achieve the tradeoff between switching and conduction loss, as shown in Fig. 7. In this design, with 400 W output power and 500 kHz switching frequency, two sets of output is selected due to its lowest total loss.

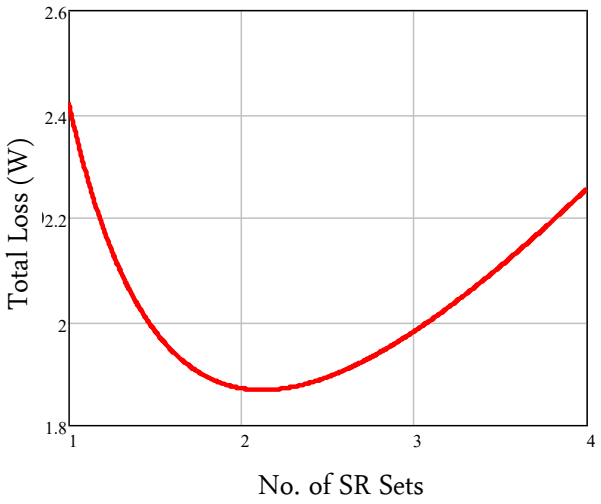

Fig. 7 Total SR loss vs. No. of SR sets.

III. Integrated Magnetic Design

The matrix transformer proves to be a promising solution for PCB-based planar transformer. By dividing the transformer into smaller parts, the number of turns for each part is reduced. Additionally, with a carefully arranged flux cancellation strategy, the core loss is effectively managed.

One challenge of the high frequency magnetic design is the strong AC effect in the windings, including the skin effect and the proximity effect, which can results to unevenly distributed current density. To mitigate this issue, interleaving between the primary and secondary windings needs to be adopted, to help minimize the high frequency AC related winding loss.

A. PCB based Matrix Transformer with Resonant Inductor Integration

Building upon the matrix transformer concept, we propose a planar transformer structure, depicted in Fig. 8. The blue line and red line denote the primary and secondary windings respectively. Fig. 9 shows the equivalent reluctance model of the proposed magnetic structure, where N_{p11} and N_{p12} refer to the primary windings on the smaller core posts (Post R), N_{p21}, N_{p22}, N_{s1} and N_{s2} correspond to the primary and secondary windings on the larger core posts (Post T). Furthermore, R_{g1} and R_{g2} represent the magnetic reluctance of the air gap on Post T and Post R, and $R_{c1} - R_{c3}$ stand for the magnetic reluctance of the core. In this proposed design, N_{p11}, N_{p12}, N_{p21} and N_{p22} are in series while N_{s1} and N_{s2} are in parallel.

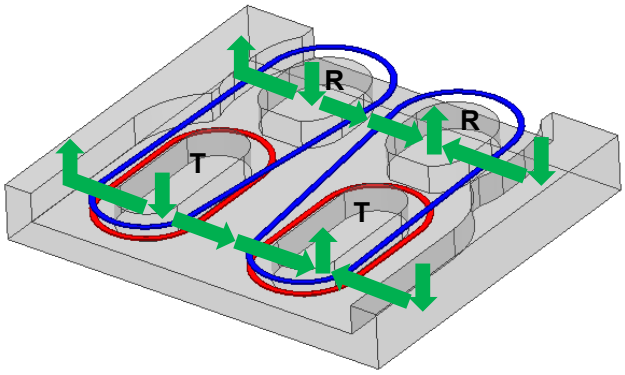

Fig. 8 Proposed matrix transformer structure with integrated resonant inductor.

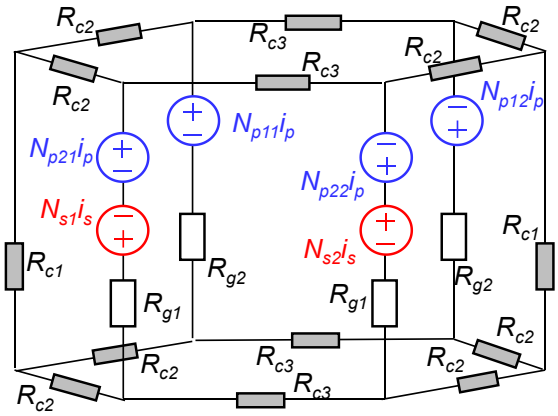

Fig. 9 Equivalent reluctance model of the proposed magnetic structure.

Based on the magnetic reluctance model, we can calculate the resonant inductance and magnetizing inductance, as shown in Eq. (4) and Eq. (5). From these simplified equations, we can see that by adjusting airgap of Post R and Post T, resonant inductance (leakage inductance in this proposed integrated magnetic structure) and magnetizing inductance can be independently changed. It is clear that Post R contributes to the resonant inductor and Post T contributes to the magnetizing inductor.

$$L_r = N_{p11}^2 \frac{(24R_{g2}^2+19R_cR_{g2}+4R_c^2)}{2R_{g2}(2R_{g2}+R_c)(3R_{g2}+R_c)} \quad (4)$$

$$L_m = N_{p21}^2 \frac{(24R_{g1}^2+19R_cR_{g1}+4R_c^2)}{2R_{g1}(2R_{g1}+R_c)(3R_{g1}+R_c)} \quad (5)$$

B. Core Loss Analysis

Another benefit of this structure is the significantly lower flux density in the core plate compared to the conventional matrix transformer [10], as demonstrated in Fig. 8. The flux not only flows in the center post (Post R and T), but also to the side posts, effectively redistributing the flux in the core plate. The 3D FEA results in Fig. 10 also show this excellent feature, in which the flux density of core plate is distributed across the whole plate and therefore becomes much lower. As a result, not only is the core loss significantly reduced, but a much lower profile is achieved by reducing the thickness of the plates.

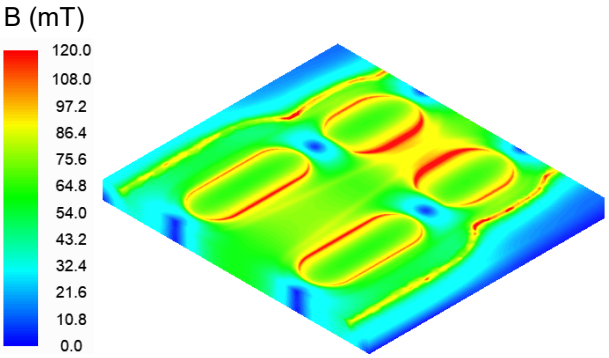

Fig. 10 Flux density distribution using 3D FEA with eddy current solver.

C. Winding Loss Analysis

The secondary side current distribution in the transformer part is shown in Fig. 11. At one time, only one set of secondary winding is conducting current due to the center-tap configuration, and from the simulation results, we can see that current is distributed relatively evenly in second windings. But still there is some current crowding at the terminations.

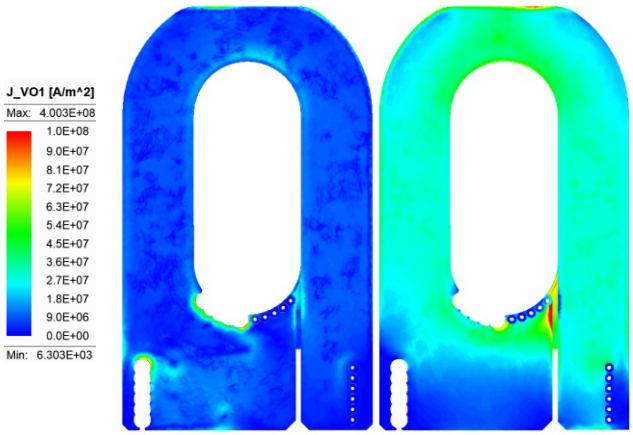

Fig. 11 Current density distribution in transformer winding (secondary side) when secondary current at its peak

The primary side current distribution in the transformer and inductor part is shown in Fig. 12. It shows that the current distribution in the transformer part is still good while in the inductor part, due to the lack of interleaving, there is some current crowding.

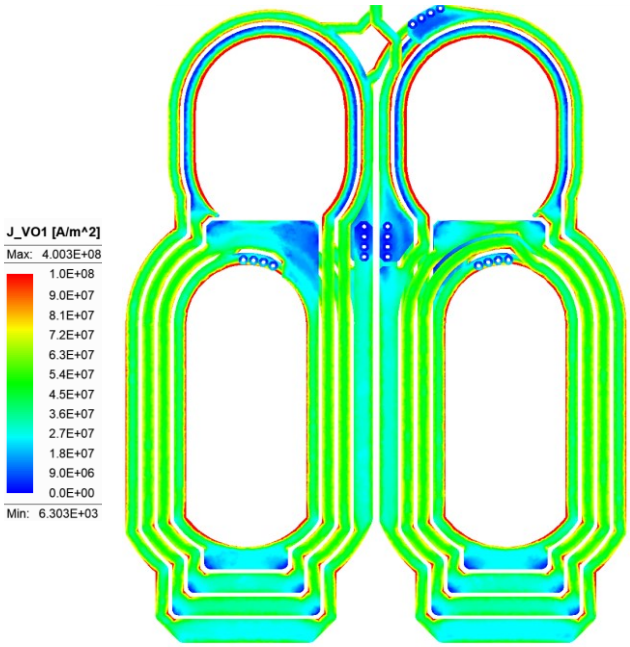

Fig. 12 Current density distribution in transformer and inductor winding (primary side) when secondary current at its peak

Winding loss distribution at 400 W is also simulated using 3D FEA with eddy current solver. Totally 8-layer PCB is used, and the results are presented in Table 1, with separated transformer loss and inductor loss in each layer.

Table 1 Winding loss distribution using 3D FEA with eddy current solver.

	Transformer	Inductor
L1 (S)	0.273W	0
L2 (S)	0.354W	0
L3	0.218W	0.013W
L4 (P)	0.768W	0.349W
L5 (P)	0.774W	0.455W
L6	0.236W	0.049W
L7 (S)	0.417W	0
L8 (S)	0.576W	0
Sum	3.616W	0.867W

From the simulation results, we can see that transformer loss dominates even at full load condition, due to the large secondary side current.

IV. Experimental Results

Based on the previous designed system structure and proposed integrated magnetic, a 400 VDC to 24 VDC, 400 W DC/DC converter module hardware prototype is built in the lab, as shown in Fig. 13. Half-bridge GaN power IC NV6247 [14] is integrated into the module, along with the resonant capacitor, output SR and output capacitors. As a result, the module only requires PWM signal and power rail input to operate.

In addition, all safety requirements are considered, especially the reinforced isolation between the primary and the secondary side (creepage distance > 7 mm), which makes sure that the prototype is good for practical applications.

An aux power supply winding is also built into the transformer, with the output voltage of 20V, it is efficient to supply most of the commercial controller ICs.

The footprint of the prototype is 62.5 x 37.2 with a maximum thickness of only 8 mm.

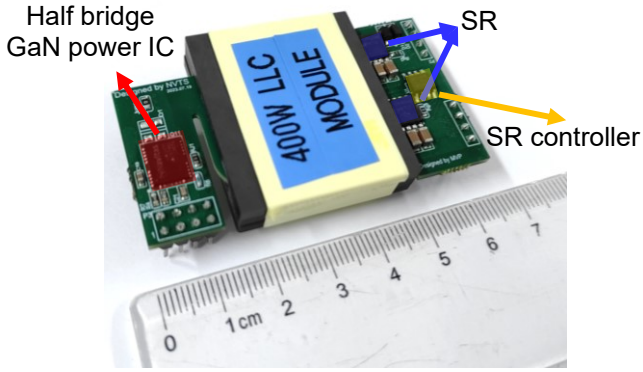

Fig. 13 Hardware prototype of the 400 W high density DC/DC module with integrated magnetic and GaN power IC.

The designed transformer parameters of the lab prototype are shown in Table 2. Magnetizing inductance is designed to have full ZVS at full load and 400 VDC input. Resonant inductance (integrated as leakage inductance) is designed with L_m/L_r ratio equals to 13 to have good regulation capability as well as system efficiency. The number of turns is determined by flux density inside the core.

The prototype is tested at 500 kHz switching frequency with up to 400 W output power. The key operation waveforms at full load are shown in Fig. 14. ZVS is achieved and the waveforms are very clean.

Table 2 Designed magnetic parameters.

Parameters	Value
$N_{p11} = N_{p12}$	3
$N_{p21} = N_{p22}$	8
N_s	2
Turns Ratio	8:1
L_r	9 uH
L_m	128 uH

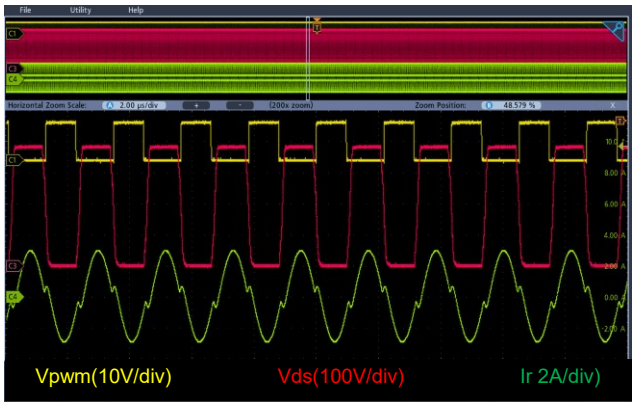

Fig. 14 steady state working waveform of the DC/DC module full load (400 W)

The tested efficiency and total system loss are shown in Fig. 15. A peak efficiency of 98.1% is achieved at around 200 W. In addition, from 180 W to 270 W, the efficiency of the DC/DC module stays above 98%. Within 350 W of output power, the total system loss stays below 10 W (including aux power supply loss).

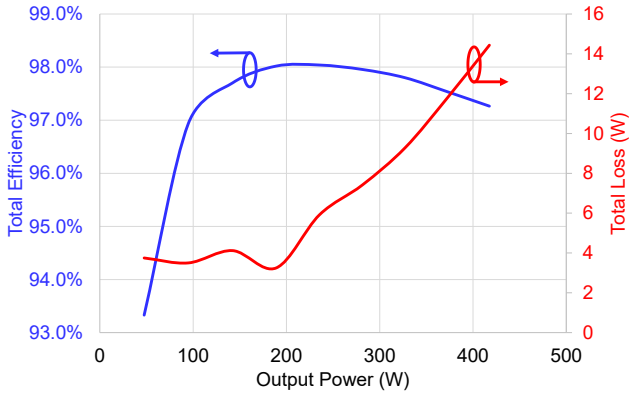

Fig. 15 Tested efficiency of the hardware prototype.

Due to the higher efficiency and lower total system loss, the prototype works well thermally even without any thermal management under natural convection at 300W, measuring maximum temperature of 98˚C on the SRIC (as shown in Fig. 16.). Due to the superior performance, the temperature of the GaN power IC is merely above 80˚C.

The hardware can also work at full load (400 W) condition if additional thermal management is implemented.

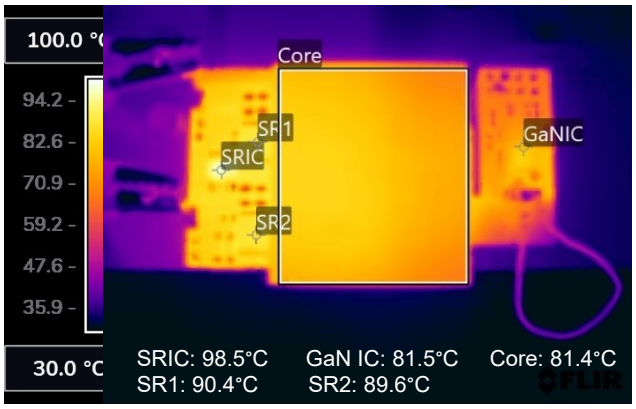

Fig. 16 Thermal performance of the DC/DC converter at 300 W under national convection and without any thermal management.

V. Conclusions and Future Work

This paper presents the design of a 400 VDC to 24 VDC 400 W DC/DC converter module serving as the second stage of the power supply in gaming laptop, portable workstation, all-in-one computer, smart display, and large screen OLED TVs. The incorporation of a half-bridge GaN power IC enables a significant reduction in the number of components and footprint required. Moreover, the implementation of a planar transformer with integrated resonant inductor further reduces the converter's size. The hardware prototype, with only 8 mm in thickness, achieved a peak efficiency of 98.1%, with a power density of 21.5 kW/L (62.5 x 37.2 x 8 mm). It worked well under natural convection with 300 W output power and can carry 400 W load once additional thermal management is implemented.

References

[1] Ribarich, T., Bredemeier, P., and Oliver, S., Gan High Density 300w Ac-Dc Converter', *PCIM Europe 2019; International Exhibition and Conference for Power Electronics, Intelligent Motion, Renewable Energy and Energy Management*, (2019)

[2] Ribarich, T. and Hodany, A., Gan Power Ics Enable 300cc 700khz 300w Ac-Dc Converter', *PCIM Europe 2023; International Exhibition and Conference for Power Electronics, Intelligent Motion, Renewable Energy and Energy Management*, (2023)

[3] Medina-Garcia, A., Krueger, M., Schmid, M., Daimer, J., and Schlenk, M., 'Hybrid-Flyback and Gan Enable Ultra-High Power Density 240w Usb-Pd Epr Adaptor', in, *2023 IEEE Applied Power Electronics Conference and Exposition (APEC)*, (2023)

[4] https://www.ifixit.com/News/58242/studio-display-teardown-is-this-secretly-an-imac, Oct. 27 2023 Accessed

[5] Huang, X., Liu, T., Li, B., Lee, F.C., and Li, Q., 'Evaluation and Applications of 600v/650v Enhancement-Mode Gan Devices', in, *Wide Bandgap Power Devices and Applications (WiPDA), 2015 IEEE 3rd Workshop on*, (2015)

[6] Fichtenbaum, N., Giandalia, M., Sharma, S., and Zhang, J., 'Half-Bridge Gan Power Ics: Performance and

Application', *IEEE Power Electronics Magazine*, 2017, 4, (3), pp. 33-40.
[7] Li, B., Huang, X., Zhang, J., Wei, T., and Zhu, J., 'High-Frequency High-Efficiency Llc Module with Planar Matrix Transformer for Crps Application Using Gan Power Ic', in, *PCIM Europe 2023; International Exhibition and Conference for Power Electronics, Intelligent Motion, Renewable Energy and Energy Management*, (2023)
[8] Li, B., Li, Q., and Lee, F.C., 'High-Frequency Pcb Winding Transformer with Integrated Inductors for a Bi-Directional Resonant Converter', *Ieee Transactions on Power Electronics*, 2019, 34, (7), pp. 6123-6135.
[9] Ouyang, Z. and Andersen, M.A., 'Overview of Planar Magnetic Technolog -- Fundamental Properties', *Power Electronics, IEEE Transactions on*, 2014, 29, (9), pp. 4888-4900.
[10] Nabih, A. and Li, Q., 'Design of 98.8% Efficient 400-to-48-V Llc Converter with Optimized Matrix Transformer and Matrix Inductor', *Ieee Transactions on Power Electronics*, 2023, 38, (6), pp. 7207-7225.
[11] Li, B., Li, Q., and Lee, F.C., 'A Novel Pcb Winding Transformer with Controllable Leakage Integration for a 6.6kw 500khz High Efficiency High Density Bi-Directional on-Board Charger', in, *2017 IEEE Applied Power Electronics Conference and Exposition (APEC)*, (2017)
[12] https://navitassemi.com/application-note-an019/, Oct. 27 2023 Accessed
[13] https://navitassemi.com/wp-content/uploads/2023/04/New-GaNSense-Half-Bridge-IC-Enables-Next-Gen-High-Frequency-High-Efficiency-High-Density-Topologies.pdf, Oct. 27 2023 Accessed
[14] https://navitassemi.com/download/, Oct. 27 2023 Accessed